



OPEN

Nonlinear Growth Kinetics of Breast Cancer Stem Cells: Implications for Cancer Stem Cell Targeted Therapy

SUBJECT AREAS:
APPLIED MATHEMATICS
BREAST CANCER
CANCER MODELS
CANCER STEM CELLS

Xinfeng Liu¹, Sara Johnson², Shou Liu², Deepak Kanojia², Wei Yue³, Udai P. Singh⁴, Qian Wang⁵, Qi Wang¹, Qing Nie^{6,7,8} & Hexin Chen²

Received
21 May 2013

Accepted
5 August 2013

Published
20 August 2013

Correspondence and requests for materials should be addressed to X.F.L. (xfliu@math.sc.edu) or H.X.C. (hchen@biol.sc.edu)

¹Department of Mathematics, University of South Carolina, Columbia, SC, 29208, ²Department of Biology, University of South Carolina, Columbia, SC, 29208, ³University of Virginia Health Sciences System, Charlottesville, Virginia, 22908, ⁴Department of Pathology, Microbiology and Immunology, School of medicine, University of South Carolina, Columbia, SC, 29208, ⁵Department of Chemistry and Biochemistry, University of South Carolina, Columbia, SC, 29208, ⁶Department of Mathematics, University of California at Irvine, Irvine, CA, 92697, ⁷Center for Mathematical and Computational Biology, University of California at Irvine, Irvine, CA, 92697, ⁸Center for Complex Biological Systems, University of California at Irvine, Irvine, CA, 92697.

Cancer stem cells (CSCs) have been identified in primary breast cancer tissues and cell lines. The CSC population varies widely among cancerous tissues and cell lines, and is often associated with aggressive breast cancers. Despite of intensive research, how the CSC population is regulated within a tumor is still not well understood so far. In this paper, we present a mathematical model to explore the growth kinetics of CSC population both *in vitro* and *in vivo*. Our mathematical models and supporting experiments suggest that there exist non-linear growth kinetics of CSCs and negative feedback mechanisms to control the balance between the population of CSCs and that of non-stem cancer cells. The model predictions can help us explain a few long-standing questions in the field of cancer stem cell research, and can be potentially used to predict the efficacy of anti-cancer therapy.

Breast cancer is a malignant disease with a heterogeneous distribution of cell types. Cancer stem cells (CSCs) are defined as ‘a small subset of cancer cells’ within a cancer that can self-renew and replenish the heterogeneous lineage of cancer cells that comprise the tumor¹. CSCs are often resistant to chemotherapeutic drugs, sharing similar gene expression profiles and properties with normal stem cells such as formation of spheres in culture, and may be responsible for tumor relapse and metastasis^{2–4}. A broad range of CSC frequency, often spanning multiple orders of magnitude, has been observed in human solid tumors of various organ types^{5–9}. CSCs isolated from primary tumors have been observed to be able to regenerate the original phenotypically heterogeneous tumors when injected into immunocompromised mice^{1,7,10}. A relevant question is how the proportion of CSC population can be maintained at a relatively constant level in tumors^{10,11}. According to the CSC hypothesis^{1,7}, CSCs possess the ability to divide either symmetrically to yield two identically immortal cancer stem cells; or asymmetrically, to simultaneously self-renew and yield one mortal non-stem cancer cell with finite replicative potential^{6,12}. The proportion of CSCs has been speculated to be maintained through alternative use of symmetric and asymmetric division¹³. However, it is largely unknown how to control the switch between these two dividing modes.

Mathematical modeling has been utilized to study underlying mechanistic principles and to help design appropriate experiments for better understanding of complex dynamics and interactions of tumor cell populations^{14–19}. Most existing models either neglect asymmetric division or progenitor cells^{17,19,20} or have made assumptions on constant division rates for CSCs with a fixed symmetric/asymmetric division probability^{14–16,21–23}. Emerging experimental data suggest that CSCs may remain quiescent or enter into an actively proliferating state²⁴. It has been reported that the relative frequency of symmetric division of CSCs changes during tumor growth¹³. Recently, a new model with two negative feedback mechanisms on the symmetric division probability and differentiation probability has been proposed¹⁹, and an excellent agreement with experimental data on the growth curve has been observed. Despite of its success on describing the growth, the model was not benchmarked against experimental dynamics on proportions of CSCs simultaneously.

In this study, we propose a mathematical model including progenitor cells (PCs) and a negative feedback on the symmetric division probability to produce two daughter cells for the next lineage to describe new



experimental observations performed both *in vitro* and *in vivo*. The mathematical model proposed in this study can fit both the growth kinetics and the proportion of CSCs *in vitro* and *in vivo* very well. In addition, we investigate the robustness and sensitivity of the models under the influence of various intrinsic and extrinsic factors and simulate potential outcomes of different therapeutic strategies for breast cancer.

Results

Cancer stem cell hypothesis as an explanation of the Gompertzian growth curve both *in vitro* and *in vivo*. It has been well-documented that the growth curve of breast cancer cells both *in vitro* and *in vivo* shows a Gompertzian shape but the underlying mechanism for the Gompertzian nature of tumor growth remains unknown^{25–27}. Here, we will explore the CSC hypothesis as an explanation for Gompertzian growth of tumors. According to the CSC hypothesis^{1,10}, breast cancer cells can be artificially divided into three main types: cancer stem cells (CSCs), progenitor cells (PCs), and terminally differentiated cells (TDCs). Cancer stem cells can divide symmetrically to produce two CSCs or two PCs, or asymmetrically to generate one CSC and

one PC. A similar mechanism applies to progenitor cells, which have limited proliferation capacity. On the other hand, TDCs lose the ability to divide further and die at predictable rate (Fig. 1a). The population dynamics of the three cell types can be described by a system of ordinary differential equations,

$$\begin{aligned}\frac{dx_0(t)}{dt} &= (p_0 - q_0)v_0x_0(t) - d_0x_0(t), \\ \frac{dx_1(t)}{dt} &= (1 - p_0 + q_0)v_0x_0(t) + (p_1 - q_1)v_1x_1(t) - d_1x_1(t), \quad (1) \\ \frac{dx_2(t)}{dt} &= (1 - p_1 + q_1)v_1x_1(t) - d_2x_2(t).\end{aligned}$$

Here we denote $x_i(t)$ the number of cells at time t for cell type i , $i = 0, 1, 2$, $p_0(p_1)$ the probability that a CSC (PC) is divided into a pair of CSCs (PCs), and $q_0(q_1)$ the probability that a CSC (PC) is divided into a pair of PCs (TDCs). Thus, $1 - p_0 - q_0$ ($1 - p_1 - q_1$) denotes the probability that an asymmetric cell division takes place from CSCs (PCs) to PCs (TDCs). Here v_0 and v_1 are the synthesis rates, which quantify how rapidly cells divide at each lineage stage in unit time, d_i , $i = 0, 1, 2$, is the degradation rate of CSCs, PCs or TDCs, respectively.

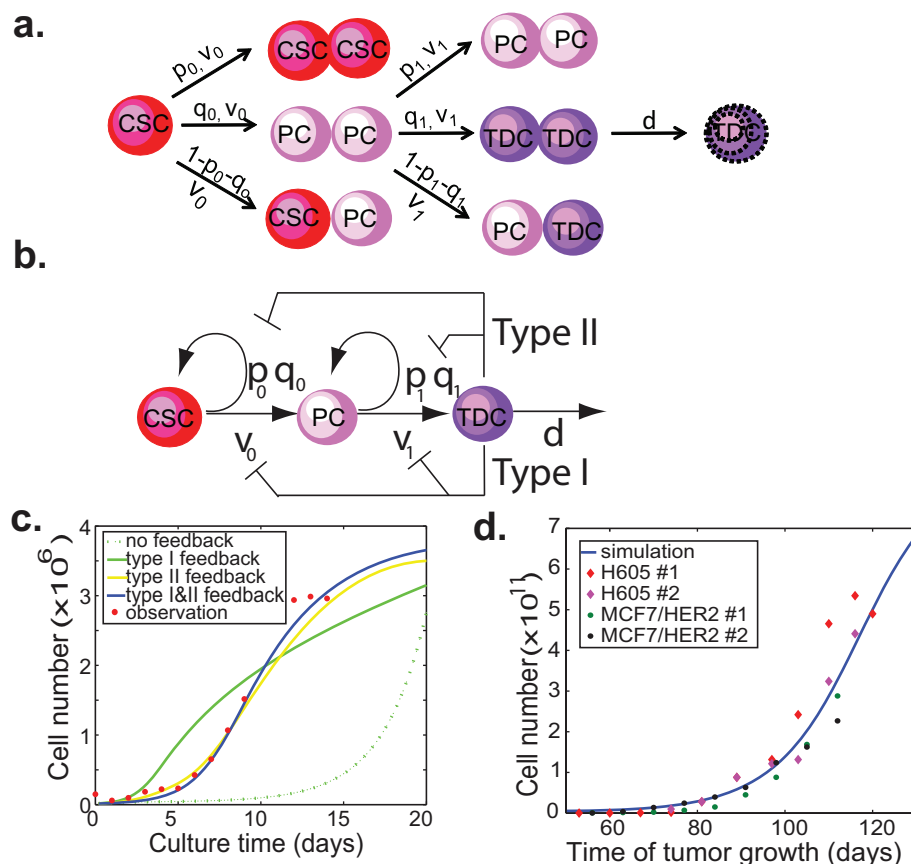


Figure 1 | Feedback regulation of symmetric division probabilities and proliferation rates of CSCs and PCs by TDCs. (a) A simple model for the proliferative kinetics of tumor cell populations. CSCs: cancer stem cells; PCs: progenitor cells; TDCs: terminally differentiated cells. The v -parameters quantify how rapidly cells divide at each linear stage. The p and q parameters quantify the fraction of symmetric division to produce two daughter cells that remain at the same stage and the next stage respectively ($1-p-q$ is the fraction of asymmetric division). d is the degradation rate of TDCs. (b) Scheme of a model with two negative feedback controls on the proliferation rates and symmetric division probabilities of CSCs and PCs by TDCs. (c) Typical simulation data of the four models in comparison with experimental data on the cell proliferation kinetics *in vitro*. MCF7 cells (1.5×10^5) are seeded in a 10-cm cell culture dish, cultured in normal conditions and counted every two days for 14 days. (d) Typical simulation data with two feedbacks compared with *in vivo* tumor growth rate. H605 mouse cells and MCF7/HER2 human breast cells (5×10^5) are injected into mammary gland of MMTV-Her2/neu syngeneic and NOD/SCID mice respectively. The tumor growth is measured using caliper weekly. There is general agreement in the literature that 1 cm^3 tumor mass contains $\sim 10^9$ cells. The tumor volume (cm^3) is estimated using the formula: tumor volume = (long axis) \times (short axis) $^2 \times \pi/6$. There are some variations in tumor initiation time points. But the tumor growth curves from all of mice show the typical Gompertzian growth pattern. Two mice selected from each group are shown in the figure. The estimated parameter values for the simulations are given in Table S2.



When this model is used to study the proliferation dynamics of tumor cells in cell culture, we find that it is very sensitive to the model parameters while the system reaches equilibrium. If $d_0 < (p_0 - q_0)v_0$ or $d_1 < (p_1 - q_1)v_1$, the number of cells will increase indefinitely, whereas the cell numbers will diminish over time if $d_0 > (p_0 - q_0)v_0$ and $d_1 > (p_1 - q_1)v_1$. In reality, the growth of breast cancer MCF7 cells *in vitro* shows a typical Gompertzian curve: a slow initial growth phase, followed by an exponential growth phase, and then a plateau phase eventually (Fig. 1c). In order for the system to reach the steady-state plateau phase, the conditions $d_0 = (p_0 - q_0)v_0$ and $d_1 < (p_1 - q_1)v_1$ must be satisfied. With these stringent conditions, the simple lineage model is unable to describe the dynamics of tumor cell growth observed *in vitro* (Fig. 1c).

Negative feedback has been shown to regulate self-renewal and proliferation of normal stem cells during organogenesis^{20,28,29}. A similar mechanism can exist for cancer cells in tumors¹⁹. To test this hypothesis, we first add feedback loops from TDCs to the division rate of CSCs and PCs in our model, denoted as Type I feedback. Specifically, we replace v_0 and v_1 by a nonlinear decreasing Hill function of the TDC population with a time delay τ and feedback strength parameters β_0 and β_1 , respectively, (also see Eq. (S2) in Supplement),

$$v_0 \rightarrow \frac{v_0}{1 + \beta_0(x_2(t - \tau))^2}, \quad v_1 \rightarrow \frac{v_1}{1 + \beta_1(x_2(t - \tau))^2}. \quad (2)$$

The hill function is generally one of the first choices for modeling feedback when there is a lack of experimental observation in responding curve^{19,20,28}. With the negative feedback, the simulated growth curve is found to describe the observed experimental data better (Fig. 1c). When we use an appropriate exponential function to model the feedback, the simulated curve also matches well with the experimental observations, but two functional forms behave differently when fitted to our observed data (Fig. S1 c–f).

Although adding Type I feedback can simulate the growth dynamics of tumor cells in culture, we wonder whether other feedback mechanisms could achieve the similar effect. Experimental data suggests that the cell population heterogeneity may also play a role in determining the growth rate of tumors both *in vitro* and *in vivo*^{2,3}. We then add a feedback from TDCs to the symmetric division probabilities of CSCs and PCs, denoted as Type II feedback. In this case, the division probabilities p_0 , q_0 , p_1 and q_1 are modeled by a nonlinear decreasing Hill function controlled by the TDC level with a time delay τ and feedback strength parameters γ (also see Eq. (S3) in Supplement),

$$p_0 \rightarrow \frac{p_0}{1 + \gamma_1^0(x_2(t - \tau))^2}, \quad q_0 \rightarrow \frac{q_0}{1 + \gamma_2^0(x_2(t - \tau))^2}, \\ p_1 \rightarrow \frac{p_1}{1 + \gamma_1^1(x_2(t - \tau))^2}, \quad q_1 \rightarrow \frac{q_1}{1 + \gamma_2^1(x_2(t - \tau))^2}. \quad (3)$$

Similar to Type I feedback, this model can also describe the experimental tumor growth data better than the one without feedback (Fig. 1c). From our observed data, we observe that very few CSC or PC cells die, suggesting a very small death rate for CSCs and PCs compared to that of TDCs. We also observe that adding the dependence of CSC or PC death rate on the fraction of TDCs does not change any of the main results (Fig. S1 a and b).

In order to test whether our model can also predict the tumor growth curve *in vivo*, we monitor the tumor growth in the transplanted animals. The growth of these tumors demonstrates that the variability is typical of malignant proliferation. For each tumor, we search for the best fitting to the observed experimental data using the least square method in L_2 norm. Examples of curves fitted to the data for two types of tumor cells are illustrated in Fig. 1d. A good agreement has been achieved for the model with two feedbacks. All the parameters are the same as in Fig. 1c except for the ones controlling

the feedback strength. Here, we find that the feedback strengths (β and γ) for both type I and II feedbacks are much weaker than the case of *in vitro* data (see Table S2). This result is consistent with previous studies showing that *in vitro* culture of primary tumor cells induces differentiation^{10,30}.

Negative feedback loops are required to control the CSC population. We next test whether the models can be applied to address another interesting phenomenon in cancer stem biology: the equilibrium between CSCs and non-cancer stem cells seems to be very robust and can be readily established after a perturbation^{10,11,15}. To test our models, we conducted two sets of experiments: 1) we culture breast cancer MCF7 cells starting at a very low density and monitor the proliferation kinetics of CSCs during the course of culture until they reach confluence; 2) we sort out the putative CSC population from MCF7/HER2 cells which contains a relatively high percentage of CSCs and monitor the differentiation process of CSCs. To test the hypothesis of the feedback on the proliferation of CSC from the differentiated cancer cells, we expect to observe different proliferation kinetics of CSCs generated from either the heterogeneous cell population or the relatively pure CSC population. The relative proportion of CSCs is measured using fluorescence-activated cell sorting (FACS) with the putative CSC makers CD44⁺CD24⁻¹⁰.

During the time course of culturing MCF7 cells, we observe that the proportion of CSCs continues to increase, reaches the peak around 5 days and then slowly goes back to the original level (Fig. S2). When we use our models to simulate the fluctuation of CSC contents during the culture course, none of the simple models including the linear model without feedback, nor the models with either Type I or Type II feedback is able to match the observed data (Fig. 2a). With a combination of both Type I and Type II feedback, however, the simulated dynamics of the CSC population agrees well with the experiments (Fig. 2a and Fig. S2a). Therefore, both Type I and Type II feedback should be included in the population dynamic model.

To further demonstrate that differentiated cells have a negative feedback on the proliferation of CSCs, we monitor the proliferation kinetics of CSCs generated from the FACS-sorted relatively pure CSC population (Fig. S2b). Without feedback, we expect that the percentage of CSC gradually decreases until that the new equilibrium is reached between CSCs and non-stem cancer cells. Surprisingly, we find that the percentage of CSCs sharply drops from 80% to 16% after two days, then slowly increases to reach the peak of 30–40% at day 8 and gradually decreases to the pre-sorting level within the following one week (Fig. 2b). Our model indicates that the parameter (τ) for the time delay should be two days, and the first phase decrease in the proportion of CSC is due to the delayed negative feedback exposed before cell sorting. This delayed negative feedback effect is released after first round of division, and the new feedback is added back to the system which contributes to the increase in the proportion of CSCs like the case of culturing MCF7 in Fig. 2a.

Overexpression of HER2 promotes either symmetric division or increases proliferation rates of CSCs, leading to expansion of the CSC population. A well-regulated biological system should be robust to genetic and environmental variations. To study sensitivity of the models to their parameters, we systematically vary the symmetric division probabilities and proliferation rates (p_0 , q_0 , v_0 , p_1 , q_1 and v_1) to exam how these changes can affect two main outputs of the system: the overall tumor cell growth and the proportion of CSCs. We find that the qualitative feature of tumor cell growth is very robust to variations of p_0 , v_0 as the growth curves agree with each other within 5% of error tolerance even when the values of p_0 , v_0 are increased by 50%. On the other hand, the tumor growth rate is very sensitive to changes of p_1 , v_1 , and the effect of p_1 on the tumor size is more prominent than that of v_1 (Fig. 3a). We next investigate the

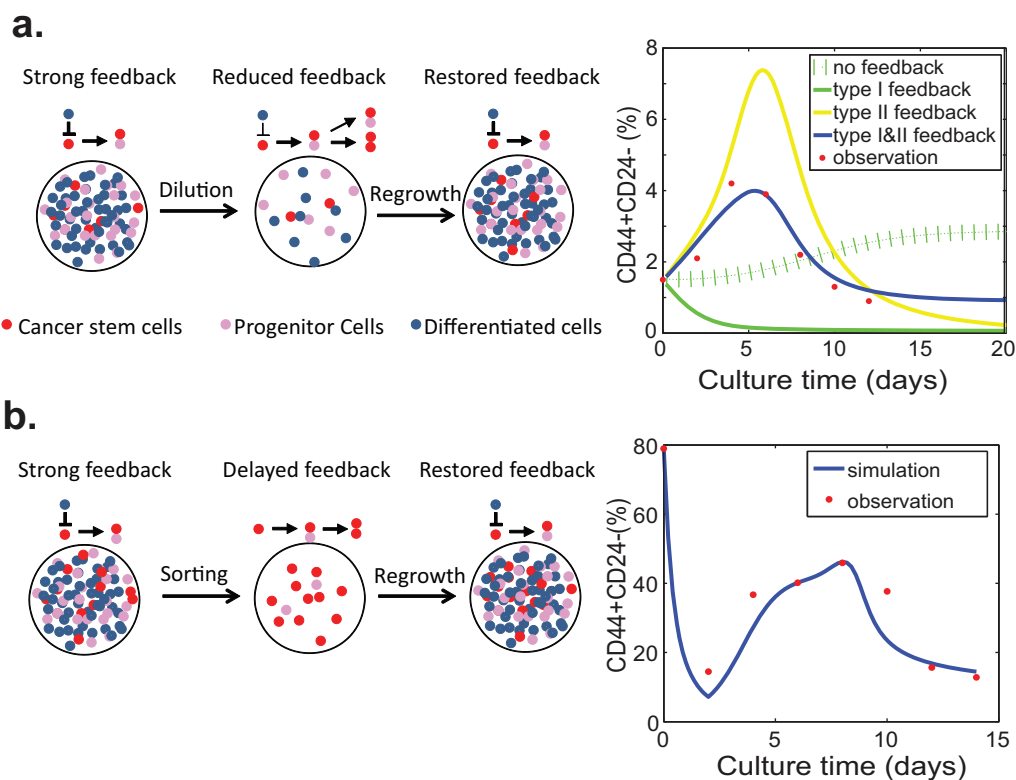


Figure 2 | Negative feedback is required for maintenance and regeneration of the equilibrium between CSCs and non-stem cancer cells.

(a) Maintenance of the relatively constant CSC population in cell culture. The cell culture is performed as described in Fig. 1C legend. The percentages of CSCs ($CD44^+CD24^-$ cells) are measured using FACS analysis every two days. (b) Regeneration of the equilibrium between CSCs and non-stem cancer cell. The putative CSCs ($CD44^+CD24^-$ cells) are sorted among MCF-7/HER2 cells by flow cytometry, and then seeded at low density (5×10^4 cells/10 cm plate) in DMEM medium containing 10% FBS. The percentages of CSCs ($CD44^+CD24^-$ cells) are measured using FACS analysis every two days. The data are shown as the means of triplicate experiments. The estimated parameter values for the simulations are given in Table S2.

effects of p_0 , v_0 , p_1 and v_1 on the relative proportion of CSCs over time (Fig. 3b). An increase in p_0 , v_0 can dramatically change the proportion of CSCs, while an increase in p_1 , v_1 reduces the proportion of CSCs. Moreover, the change in p_0 has a more dramatic effect than that in v_0 .

To test negative feedback mechanisms predicted by the model experimentally, we investigate how the genetic perturbation can affect the dynamic change in cancer cell subpopulations. Oncogene HER2 is a well-studied oncogene known for its role in promoting cancer cell survival and proliferation, and recently implicated in generation and maintenance of CSCs^{31,32}. We examine the consequence of HER2 overexpression in breast cancer cell line MCF7. Western blot analysis results show that HER2 signaling is activated in MCF7-HER2 cells (Fig. S3). Intriguingly, we observe that overexpression of HER2 in MCF7 cells has no effect on the growth kinetics of the total cell population (Fig. 3c), but can result in an almost 13-fold increase in the $CD44^+CD24^-$ cell population ($11.4 \pm 1.5\%$ vs. $0.9 \pm 0.3\%$) (Fig. 3d), which is the putative CSC population¹⁰. Apparently, overexpression of HER2 doesn't generate the feedback aimed at p_1 and/or v_1 because changes in p_1 and/or v_1 can, in theory, produce more visible effect on the growth kinetics of tumor cells. Given that negative feedback aimed at either v_0 (division rate) or p_0 (self-renewal probability) can lead to dramatic changes in the proportion of CSCs, it is likely that overexpression of HER2 increases v_0 and/or p_0 . This possibility is supported by a recent finding that HER2 overexpression in mammary CSCs increases the frequency of self-renewal division¹³.

Majority of tumorspheres are generated from PCs instead of CSCs. The equilibrium between CSCs and non-stem CSCs may be

disturbed by extrinsic factors such as culture conditions. Tumorsphere culture has been widely used to enrich and culture CSCs from a variety of cancers including the breast cancer^{33,34}. Since tumorspheres are cultured in a suspension medium without serum, the majority of non-stem cancer cells die within the first 24–48 hours. Presumably, all CSCs and partial PCs can survive these harsh conditions and then proliferate to form tumorspheres after a certain period of culture. Our previous data show that primary tumor cells derived from *MMTV-Her2* transgenic mice can be cultured as tumorspheres for more than twenty passages³⁵. We observe that tumorsphere-forming efficiency gradually increases over the early passages, reaching a plateau after passage 11 (Fig. 4b)³⁵. Similar phenomena have been reported for other cell lines in the literature^{36,37}. It is widely speculated that the increase in tumorsphere-forming efficiency is positively correlated to the proportion of CSCs. Here we use the model with a combination of Type I and II feedback (Eq. (S4) in Supplement) to quantitatively show how the subpopulation of cells evolves over the passages of tumorsphere in culture.

Our model uncovers several unanticipated results in such temporal courses. First, even though the proportion of CSCs shows a sharp increase in the first generation of tumorspheres, it cannot continue to increase over the tumorsphere passages. To the contrary, the proportion of CSCs dramatically decreases after 8 ~ 10 passages of tumorsphere culture (Fig. 4c). We test this prediction by evaluating the tumorigenicity of tumorspheric cells at different passages in syngeneic animals. We observe that the proportion of CSCs in the first generation of tumorspheres is enriched by about 30-fold; in the meantime, the tumorigenicity of tumorspheres decreases gradually with continuous tumorsphere culture (Table 1).

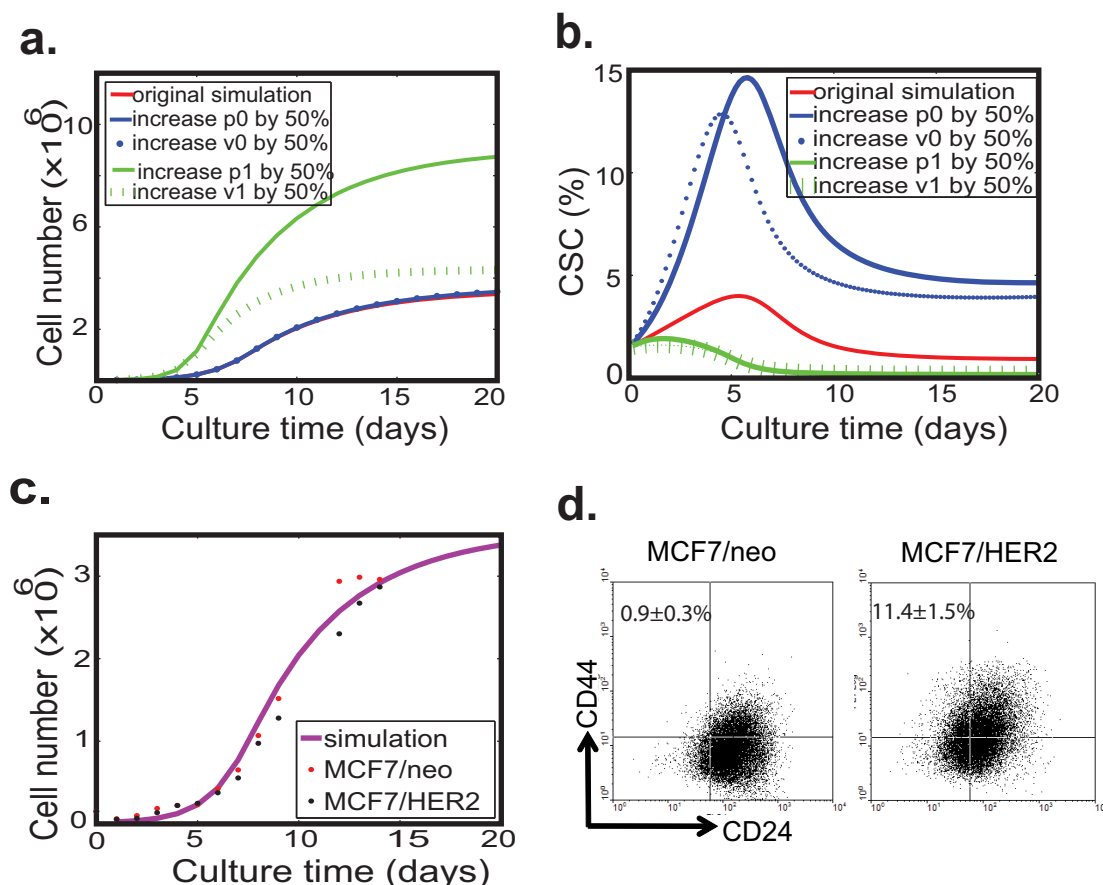


Figure 3 | Robustness of the model with a combination of Type I & II negative feedback loops. (a) The simulated total cell number profile is robust to variations of v_0 and p_0 , but is sensitive to variations of v_1 and p_1 . (b) The simulations show that an increase in v_0 or p_0 boosts the relative proportion of CSCs, while an increase in v_1 or p_1 reduces the proportion of CSCs. (c) Simulated growth curve of HER2-overexpressing MCF7 cells and control cells matches the experimental data. MCF7 cells are plated in 6 well plates and the cell culture medium is replaced with fresh medium every 2 days. At the desired moment, cells are harvested and counted by trypan blue exclusion assay. The experiments were performed in triplicate. (d) FACS analysis of the putative CSC population in HER2-overexpressing MCF7 cells and control cells. Overexpression of HER2 resulted in about 10-fold increase in the CD44⁺CD24⁻ population. The estimated parameter values for the simulations are given in Table S2.

The apparent paradox between increased tumorsphere-forming efficiency and decreased tumorigenicity of high-passages tumorspheres can be explained effectively by the model: both CSCs and some PCs can form tumorspheres, and moreover, the majority of tumorspheres, at least in our experimental model system, are derived from PCs. The proportion of PC-derived tumorspheres gradually increases upon continuous passages while the proportion of CSC-derived tumorspheres progressively decreases (Table S1). The dynamic changes in the proportion of both CSCs and PCs are largely due to the depletion of differentiated tumor cells and readjustment of the equilibrium between CSCs and non-stem cancer cells.

CSC-targeted drug is a better choice for long-term maintenance therapy. The CSC hypothesis may be of particular importance because of the observed resistance of CSCs to chemo- and radiation therapies^{38,39}. The mathematical model with both Type I and II feedback can be used to study correlations among tumor size, proportion of CSCs and tumor relapse after cancer treatment. Our model studies suggest that CSC-targeted therapy is less effective in shrinkage of tumor size but more effective in long-time suppression of tumor growth and prevention of tumor relapse (Fig. 5a and 5b). In contrast, conventional chemotherapies may cause dramatic tumor shrinkage but a sharp increase in the CSC population (Fig. 5b), presumably due to the killing of TDCs and the relief of negative feedback. To validate this prediction, we assume that the death

rates of PCs and TDCs will be tripled for the case of standard chemotherapy (e.g. doxorubicin) compared to the system without drug treatment, and the feedback strengths for two feedbacks are maintained the same as the case shown in Fig. 1d (see Table S2). Our computation shows that conventional chemotherapies result in a sharp increase in the CSC percentage, which is in agreement with the clinical data reported by Li et al (Fig. 5c)⁴⁰. Since HER2 signaling is critical for self-renewal of CSCs^{13,32}, HER2-targeted therapy (e.g. lapatinib treatment) may preferentially target CSCs. So we vary the parameter that decides division pattern of CSCs when the lapatinib treatment is imposed. As a first approximation, we simply reduce the value of p_0 from 0.5 to 0.3. The simulated results are shown in Fig. 5d, where the blue solid line represents the percentage of CSCs during the course of treatment. Consistent with the observed clinical data, lapatinib treatment leads to a decrease in the percentage of CSCs (Fig. 5d). We don't observe the sharp decrease in the percentage of CSC partially because lapatinib can inhibit the growth of PCs and TDCs as well.

It is generally believed that combined treatment targeting both CSCs and non-stem cancer cells will be the best choice for cancer patient. Interestingly, our simulation results reveal that CSC-targeted therapy can achieve better long-term clinical outcomes compared to combined treatment targeting at both CSCs and non-CSCs (Fig. 5a and 5b). Especially after the long-time maintenance treatment, the tumor volume decreases for a certain period of time (Fig. 5a).

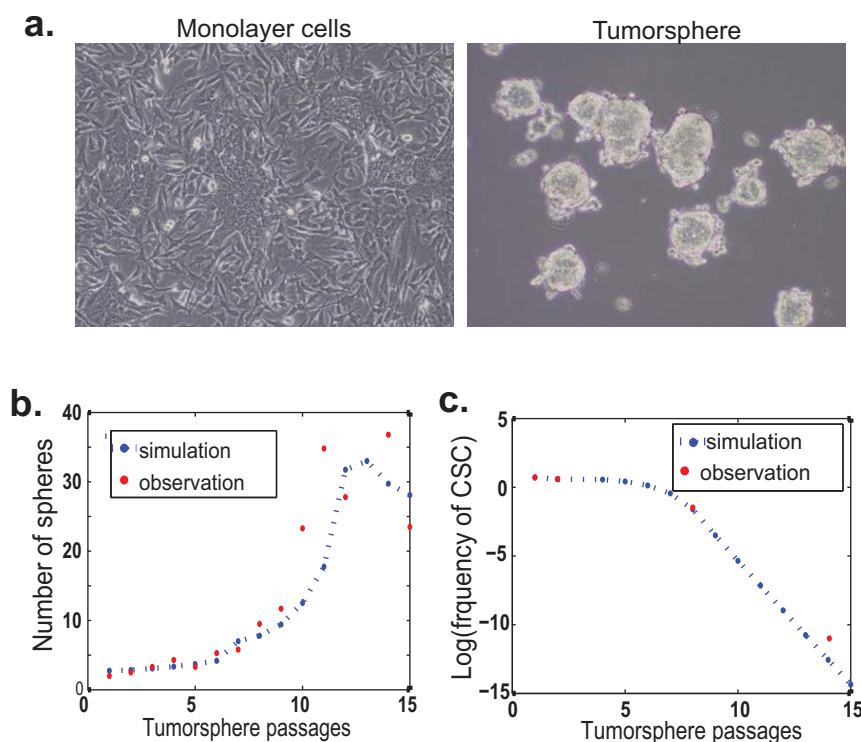


Figure 4 | Dynamic change of CSC population during tumorsphere formation and propagation. (a) Microscopy examination of MMTV-Her2/neu primary tumor cells cultured under adherent and suspension conditions. (b) Simulated number of continuously passaged tumorspheres using the mathematical model with two feedback controls matches the experiment very well. (c) Simulated frequency of CSCs during the passages for tumorsphere formation matches the observed data. The observed and predicted frequencies of CSC are listed in Table S1. The estimated parameter values for the simulations are given in Table S2.

However, when the treatment stops, tumors treated with combined therapies will relapse faster than the tumors treated with CSC-targeted therapy. The explanation for this prediction is that reduction in the numbers of PCs and TDCs with conventional therapy leads to a shift from asymmetric to symmetric division or increase the proliferation rate of the remaining CSCs.

We also test the situation in which CSCs could be selectively targeted for destruction by increasing the destruction rate for CSC targeted therapy, and find the overall response pattern is similar to the early drug response (Fig. S4). However, the increased tumor cell-killing activity may be associated with increased toxicity in clinical situations, and it remains to be validated on whether complete remission as a result of CSC-targeted therapy alone is achievable in practice.

Discussion

In this paper, we develop a set of mathematical models for studying the dynamic interaction between CSCs and non-stem cancer cells. After benchmarking against direct tissue culture experiments and xenograft transplantation assays, we conclude that the appropriate model needs negative feedbacks on both division rates (Type I) and self-renewal probabilities (Type II) in order to obtain the experimentally observed balance between CSCs and non-stem cancer cells. This study suggests that CSCs alone are more likely to undergo symmetric division (self-renewal) at a higher proliferation rate; whereas CSCs directly or indirectly interacted with differentiated cancer cells are likely to undergo asymmetric division at a lower proliferation rate. This dynamic interaction between CSCs and non-stem cancer cells eventually determine the proportion of CSCs within a tumor.

Our mathematical model provides an explanation for the question why in xenograft transplantation assays the CSC content of the minimum cell dose for tumor growth is usually 10 times higher than that is required when sorted CSCs are used^{10,30,41}. According to our models, TDCs impose a negative feedback on the self-renewal probability and/or proliferation rate of CSCs, therefore inhibit tumor initiation when unsorted bulky cells are used for injection. Since only live TDCs are capable of executing these negative feedback effects, our models do not apply to many other studies of tumor transplantation in syngeneic animal models, in which adding lethally irradiated tumor cells to the injected cell population reduces the number of cells required to cause tumor growth^{42,43}. In this case, the dead cells cannot maintain the functional interaction with CSCs but instead may release cellular components that stimulate an inflammatory response, which is well known to promote tumor growth^{36,44}.

Another interesting phenomenon is that CSCs isolated from either primary tissues or cell lines can rapidly regenerate the original

Table 1 | Tumor formation capability of adherent cells and continuously passaged tumorspheres

| No. of injected cells | Adherent culture | Serial passages of tumorspheres | | | |
|-----------------------|------------------|---------------------------------|-----|-----|-----|
| | | P1 | P2 | P8 | P14 |
| 50 | NA | 3/8 | NA | NA | NA |
| 100 | 0/4 | 4/4 | 3/4 | 3/4 | NA |
| 500 | 0/4 | 8/8 | NA | NA | 0/4 |
| 1,000 | 0/4 | N/A | 4/4 | 4/4 | 0/4 |
| 5,000 | 4/4 | 4/4 | 4/4 | 3/4 | 0/4 |
| 10,000 | 2/2 | NA | 2/2 | NA | 1/2 |

After injection into the mammary fat pads of syngeneic mice at different concentrations, mice were examined weekly for tumors by observation and palpation. The number of tumors formed and the number of injections performed are indicated for each population at 12 weeks. NA: not available.

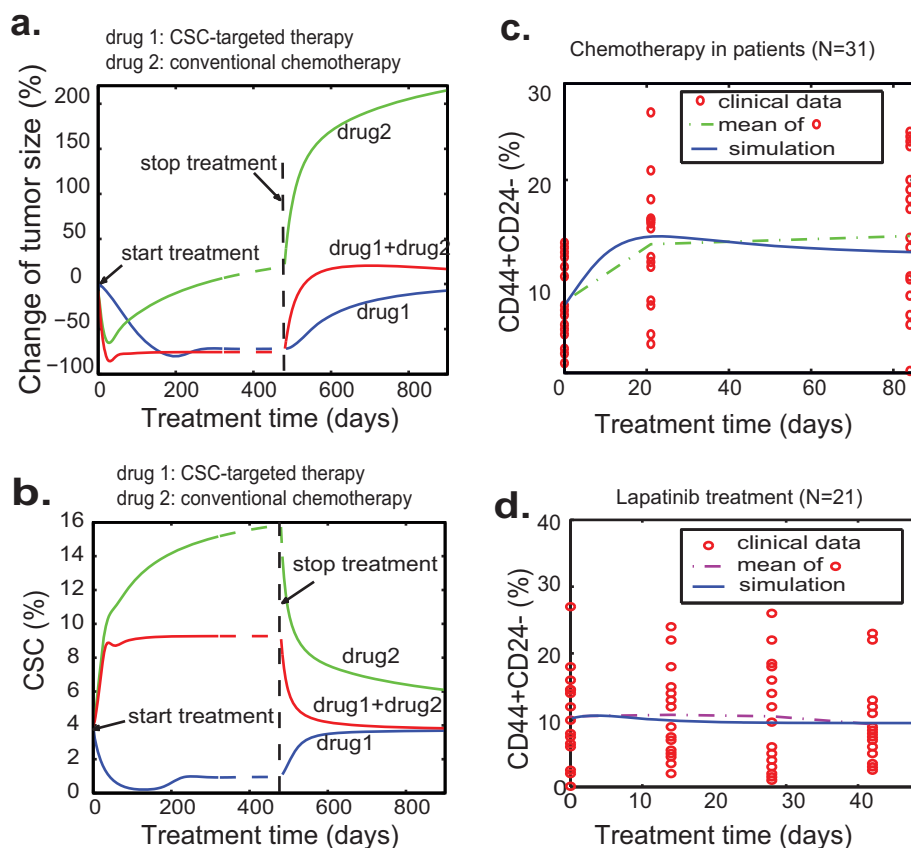


Figure 5 | Simulated tumor responses to different anti-cancer drug treatments and with a comparison to clinical data. (a) Simulated tumor size changes with three different treatment strategies: CSC-targeted therapy, conventional chemotherapy and combination of these two. (b) The dynamics of the proportion of CSCs with three different treatment strategies. (c–d) Simulated percentage of CSCs compared to clinical data with two drug treatment strategies. The simulated curves agree well with the mean curves of clinical data. The percentages of CD44⁺CD24⁻ cells represent the CSCs in primary tumors under the treatment of conventional chemotherapy and dual EGFR/HER2 inhibitor lapatinib. The clinical data on chemotherapy and lapatinib treatment is derived from⁴⁰. The estimated parameter values for the simulations are given in Table S2.

heterogeneity and maintain it at a relatively constant level^{10,11}. Recently, several studies suggested that CSCs may arise from non-cancer stem cells randomly or induced by microenvironmental factors via an EMT process^{11,45}. To maintain a stable equilibrium, the rate of CSC differentiation must be balanced by the rate of CSC formation through constant self-renewal of CSCs and conversion from non-stem cancer cells^{11,15}. Interestingly, simulations of our mathematical models show that a very strict condition on model parameters (Eq. (S6)) must be imposed in order for the cell population to reach an equilibrium state (also see Fig. S7).

Sphere culture, which was introduced to isolate and expand neural stem cells, has been adopted to enrich and quantify the frequency of CSCs in a variety of primary tumor cells or cancer cell lines³⁴. The premise for this assay is that most if not all tumorspheres are derived from CSCs. It is often observed that the differences between the frequency of tumorsphere formation and the frequency of tumor-initiation in a xenograft assay range from a few percent to several orders of magnitude^{38,41,45}. These differences are explained based on the belief that not every single CSC can survive and grow into a tumor in the transplanted animals. If the *in-vivo* transplantation assay accurately reflects the frequency of CSCs, another alternative explanation is that not all tumorspheres are derived from CSCs. Actually it has been shown that the majority (>90%) of neural spheres are not stem-cell derived²¹. If the majority of tumorspheres are derived from PCs, our model provides a clear explanation for the apparently paradoxical observation that, in the continuously

passed tumorspheres, the frequency of tumorsphere formation increases but the frequency of CSCs decreases (Table S1). Similarly, we can also explain why tumorsphere culture cannot always be used to enrich CSCs from all tumor cell lines⁴⁶. According to our model studies, the proportion of CSCs during tumorsphere culture is determined by two critical factors: the self-renewal frequency of CSCs during each tumorsphere formation and the ratio of tumorspheres derived from CSCs or PCs.

Finally, our models may have some clinical applications such as predicting the efficacy of anti-cancer therapy. The CSC hypothesis suggests that a cure for cancer should include the complete loss of cancer stem cell function^{47,48}. Current therapeutic strategies preferentially target at non-stem cancer cells, underscoring the need for developing CSC-specific therapies. It is generally believed that the optimal therapeutic regimen is needed to target at both CSCs and non-CSCs. The relevant question is whether combinations of multiple drugs always achieve better results than a single drug treatment. If non-CSCs can indeed negatively affect the self-renewal of CSCs as our model suggests, removal of non-CSCs by non-CSC targeting conventional therapy can relieve the negative feedback regulation, leading to enhancement of self-renewal of CSCs. Consistent with our modeling results, the dramatic increase in the proportion of CSCs after conventional chemotherapies has been reported³⁸. Another surprising result of our model studies is that CSC-targeted drugs can eventually do a better job to inhibit tumor growth and to prevent tumor relapse than a combination of drugs that target at both CSCs



and non-CSCs if no drug-resistant mutations occur. This prediction, if justified *in vivo*, will have a significant implication to the development of anti-cancer therapies.

Methods

Cell culture and proliferation analysis. MCF7/neo and MCF/HER2-18 cell lines (kindly provided by Dr. Rachel Schiff at the Baylor College of Medicine) were grown in DMEM/F12 medium supplemented with 10% FBS and 5 $\mu\text{g/ml}$ insulin⁴⁹. Cells were cultured at 37°C in a humidified atmosphere containing 5% CO₂.

Isolation and culture of cancer cells from MMTV-Neu transgenic mouse mammary tumors. Isolation and culture of cancer epithelial cells from mammary tumors of MMTV-*Her2/neu*-transgenic mice were described previously⁵⁰. In short spontaneous mammary tumors that developed from MMTV-Neu transgenic mice were harvested, and digested in DMEM/F12 medium with 1.5 mg/ml collagenase (Worthington) and 20 $\mu\text{g/ml}$ hyaluronidase (MP Biomedicals) for 2 hours at 37°C. The pellet was resuspended in DMEM/F12 medium and passed through a 40 μm strainer (PALL Corporation) to collect single cells. The Lin⁻ epithelial cells were enriched by removing CD45⁺/Ter119⁺, CD31⁺ and CD140a⁺ cells using antibodies against those respective surface antigens and the EasySep magnet (StemCell Technologies, Vancouver, BC, Canada) according to the manufacturer's instructions. The isolated cells were maintained in Dulbecco's modified Eagle's medium (DMEM, Gibco) with 10% fetal-bovine serum (FBS, SAFC Biosciences) and 10 $\mu\text{g/ml}$ insulin (Sigma) as differentiated cancer cells.

In vitro propagation of tumorspheres. Cells harvested from spontaneous tumors were cultured in ultra-low attachment 6-well plates (Corning, Acton, MA, USA) at a density of 5000 cells/ml in serum-free DMEM/F12 medium (Invitrogen) supplemented with 20 ng/ml epidermal growth factor (EGF, Sigma, St. Louis, MO, USA), 10 ng/ml basic fibroblast growth factor (bFGF, Sigma), 5 $\mu\text{g/ml}$ insulin (Sigma), 1 \times B27 supplement (Invitrogen) and 0.4% bovine serum albumin (BSA, Sigma).

Flow cytometry analysis. Fluorescence-activated cell sorting (FACS) analysis was performed using an FC500 CXP flow cytometer (Beckman Coulter, Fullerton, CA, USA). Cells were stained with the following antibodies: PE-conjugated anti-CD24 and FITC-conjugated anti-CD44 (BioLegend, San Diego, CA, USA). Cell sorting was carried out on a FACSAria II cell sorter (Becton Dickinson).

In vivo tumorigenesis assays. Cells were resuspended in 20 μl DMEM/F12 medium and mixed with 20 μl Matrigel (Becton Dickinson) at a 1 : 1 ratio and held on ice. The entire 40 μl sample was injected into either no.4 mammary glands of MMTV-*Her2/neu*-transgenic and NOD/SCID mice anesthetized with isoflurane according to the animal protocol approved by the USC committee for research in vertebrate animals. Tumor sizes were measured weekly. Incidence of xenograft tumor formation was scored 12–13 weeks after injection.

Statistical analysis. Data were expressed as the mean (standard deviation (SD)). Differences between any two groups were determined by ANOVA. $P < 0.05$ was considered statistically significant.

Parameter fitting procedure. A range of parameters in the model is first chosen. Many values of each parameter are then uniformly and randomly sampled within the range to compute the numbers of CSCs, PCs, and TDCs in the model. The case that has the minimal least square error with $L2$ norm between the simulation and the observed data is considered as the best fit. For example, for the model with two feedbacks in Fig. 1C, the range of p_0 is between 0 and 1, q_0 is between 0 and 1 – p_0 after p_0 is chosen, the feedback strength γ is between 10^{-13} and 10^{-16} , β is between 10^{-13} and 10^{-11} , and five values of each parameter are uniformly selected in the given range to perform the simulations.

- Clarke, M. F. *et al.* Cancer stem cells—perspectives on current status and future directions: AACR Workshop on cancer stem cells. *Cancer Res.* **66**, 9339–9344 (2006).
- Shipitsin, M. *et al.* Molecular definition of breast tumor heterogeneity. *Cancer Cell* **11**, 259–273 (2007).
- Pece, S. *et al.* Biological and molecular heterogeneity of breast cancers correlates with their cancer stem cell content. *Cell* **140**, 62–73 (2010).
- Ben-Porath, I. *et al.* An embryonic stem cell-like gene expression signature in poorly differentiated aggressive human tumors. *Nat. Genet.* **40**, 499–507 (2008).
- Visvader, J. E. & Lindeman, G. J. Cancer stem cells in solid tumours: accumulating evidence and unresolved questions. *Nat. Rev. Cancer* **8**, 755–768 (2008).
- Tan, B. T., Park, C. Y., Ailles, L. E. & Weissman, I. L. The cancer stem cell hypothesis: a work in progress. *Lab. Invest.* **86**, 1203–1207 (2006).
- Dalerba, P., Cho, R. W. & Clarke, M. F. Cancer stem cells: models and concepts. *Annu. Rev. Med.* **58**, 267–284 (2007).
- Hill, R. P. & Parris, R. "Destemming" cancer stem cells. *J. Natl. Cancer Inst.* **99**, 1435–1440 (2007).
- Lobo, N. A., Shimono, Y., Qian, D. & Clarke, M. F. The biology of cancer stem cells. *Annu. Rev. Cell Dev. Biol.* **23**, 675–699 (2007).
- Al-Hajj, M., Wicha, M. S., Benito-Hernandez, A., Morrison, S. J. & Clarke, M. F. Prospective identification of tumorigenic breast cancer cells. *Proc. Natl. Acad. Sci. U. S. A.* **100**, 3983–3988 (2003).
- Iliopoulos, D., Hirsch, H. A., Wang, G. & Struhl, K. Inducible formation of breast cancer stem cells and their dynamic equilibrium with non-stem cancer cells via IL6 secretion. *Proc. Natl. Acad. Sci. U. S. A.* **108**, 1397–1402 (2011).
- Ailles, L. E. & Weissman, I. L. Cancer stem cells in solid tumors. *Curr. Opin. Biotechnol.* **18**, 460–466 (2007).
- Cicalese, A. *et al.* The tumor suppressor p53 regulates polarity of self-renewing divisions in mammary stem cells. *Cell* **138**, 1083–1095 (2009).
- Mackillop, W. J., Ciampi, A., Till, J. E. & Buick, R. N. A stem cell model of human tumor growth: implications for tumor cell clonogenic assays. *J. Natl. Cancer Inst.* **70**, 9–16 (1983).
- Gupta, P. B. *et al.* Stochastic state transitions give rise to phenotypic equilibrium in populations of cancer cells. *Cell* **146**, 633–644 (2011).
- Boman, B. M., Wicha, M. S., Fields, J. Z. & Runquist, O. A. Symmetric division of cancer stem cells—a key mechanism in tumor growth that should be targeted in future therapeutic approaches. *Clin. Pharmacol. Ther.* **81**, 893–898 (2007).
- Sehl, M. E., Sinsheimer, J. S., Zhou, H. & Lange, K. L. Differential destruction of stem cells: implications for targeted cancer stem cell therapy. *Cancer Res.* **69**, 9481–9489 (2009).
- Zhu, X., Zhou, X., Lewis, M. T., Xia, L. & Wong, S. Cancer stem cell, niche and EGFR decide tumor development and treatment response: A bio-computational simulation study. *J. Theor. Biol.* **269**, 138–149 (2010).
- Rodriguez-Brenes, I. A., Komarova, N. L. & Wodarz, D. Evolutionary dynamics of feedback escape and the development of stem-cell-driven cancers. *Proc. Natl. Acad. Sci. U. S. A.* **108**, 18983–18988 (2011).
- Lander, A. D., Gokoffski, K. K., Wan, F. Y., Nie, Q. & Calof, A. L. Cell lineages and the logic of proliferative control. *PLoS Biol.* **7**, e15 (2009).
- Deleyrolle, L. P. *et al.* Determination of somatic and cancer stem cell self-renewing symmetric division rate using sphere assays. *PLoS ONE* **6**, e15844 (2011).
- Selby, P., Bizzari, J. P. & Buick, R. N. Therapeutic implications of a stem cell model for human breast cancer: a hypothesis. *Cancer Treat. Rep.* **67**, 659–663 (1983).
- Morton, C. I., Hlatky, L., Hahnfeldt, P. & Enderling, H. Non-stem cancer cell kinetics modulate solid tumor progression. *Theor. Biol. Med. Model.* **8**, 48 (2011).
- Schober, M. & Fuchs, E. Tumor-initiating stem cells of squamous cell carcinomas and their control by TGF-beta and integrin/focal adhesion kinase (FAK) signaling. *Proc. Natl. Acad. Sci. U. S. A.* **108**, 10544–10549 (2011).
- Norton, L., Simon, R., Brereton, H. D. & Bogden, A. E. Predicting the course of Gompertzian growth. *Nature* **264**, 542–545 (1976).
- Norton, L. A Gompertzian model of human breast cancer growth. *Cancer Res.* **48**, 7067–7071 (1988).
- Brunner, N. *et al.* Characterization of the T61 human breast carcinoma established in nude mice. *Eur. J. Cancer Clin. Oncol.* **21**, 833–843 (1985).
- Lo, W. C. *et al.* Feedback regulation in multistage cell lineages. *Math. Biosci. Eng.* **6**, 59–82 (2009).
- Johnston, M. D., Edwards, C. M., Bodmer, W. F., Maini, P. K. & Chapman, S. J. Mathematical modeling of cell population dynamics in the colonic crypt and in colorectal cancer. *Proc. Natl. Acad. Sci. U. S. A.* **104**, 4008–4013 (2007).
- O'Brien, C. A., Pollett, A., Gallinger, S. & Dick, J. E. A human colon cancer cell capable of initiating tumour growth in immunodeficient mice. *Nature* **445**, 106–110 (2007).
- Magnifico, A. *et al.* Tumor-initiating cells of HER2-positive carcinoma cell lines express the highest oncoprotein levels and are sensitive to trastuzumab. *Clin. Cancer Res.* **15**, 2010–2021 (2009).
- Korkaya, H., Paulson, A., Iovino, F. & Wicha, M. S. HER2 regulates the mammary stem/progenitor cell population driving tumorigenesis and invasion. *Oncogene* **27**, 6120–6130 (2008).
- Dontu, G. *et al.* In vitro propagation and transcriptional profiling of human mammary stem/progenitor cells. *Genes Dev.* **17**, 1253–1270 (2003).
- Dontu, G. & Wicha, M. S. Survival of mammary stem cells in suspension culture: implications for stem cell biology and neoplasia. *J. Mammary Gland Biol. Neoplasia* **10**, 75–86 (2005).
- Gu, Y. *et al.* The effect of B27 supplement on promoting in vitro propagation of Her2/neu-transformed mammary tumorspheres. *J. Biotech. Res.* **3**, 7–18 (2011).
- Iliopoulos, D., Hirsch, H. A. & Struhl, K. An epigenetic switch involving NF-kappaB, Lin28, Let-7 MicroRNA, and IL6 links inflammation to cell transformation. *Cell* **139**, 693–706 (2009).
- Cariati, M. *et al.* Alpha-6 integrin is necessary for the tumorigenicity of a stem cell-like subpopulation within the MCF7 breast cancer cell line. *Int. J. Cancer* **122**, 298–304 (2008).
- Yu, F. *et al.* let-7 regulates self renewal and tumorigenicity of breast cancer cells. *Cell* **131**, 1109–1123 (2007).
- Bao, S. *et al.* Glioma stem cells promote radioresistance by preferential activation of the DNA damage response. *Nature* **444**, 756–760 (2006).
- Li, X. *et al.* Intrinsic resistance of tumorigenic breast cancer cells to chemotherapy. *J. Natl. Cancer Inst.* **100**, 672–679 (2008).
- Ricci-Vitiani, L. *et al.* Identification and expansion of human colon-cancer-initiating cells. *Nature* **445**, 111–115 (2007).
- Steel, G. G., Adams, K. & Stephens, T. C. Clonogenic assays in the B16 melanoma: response to cyclophosphamide. *Br. J. Cancer* **36**, 618–624 (1977).



43. Hewitt, H. B., Blake, E. & Proter, E. H. The effect of lethally irradiated cells on the transplantability of murine tumours. *Br. J. Cancer* **28**, 123–135 (1973).
44. Scheel, C. *et al.* Paracrine and autocrine signals induce and maintain mesenchymal and stem cell states in the breast. *Cell* **145**, 926–940.
45. Mani, S. A. *et al.* The epithelial-mesenchymal transition generates cells with properties of stem cells. *Cell* **133**, 704–715 (2008).
46. Stuelten, C. H. *et al.* Complex display of putative tumor stem cell markers in the NCI60 tumor cell line panel. *Stem cells* **28**, 649–660 (2010).
47. Norton, L. Cancer stem cells, self-seeding, and decremented exponential growth: theoretical and clinical implications. *Breast Dis.* **29**, 27–36 (2008).
48. Norton, L. Conceptual and practical implications of breast tissue geometry: toward a more effective, less toxic therapy. *The oncologist* **10**, 370–381 (2005).
49. Benz, C. C. *et al.* Estrogen-dependent, tamoxifen-resistant tumorigenic growth of MCF-7 cells transfected with HER2/neu. *Breast Cancer Res. Treat.* **24**, 85–95 (1992).
50. Chen, H. *et al.* Proteomic characterization of Her2/neu-overexpressing breast cancer cells. *Proteomics* **10**, 3800–3810 (2010).

Acknowledgments

The authors thank Dr. Rachel Schiff at the Baylor College of Medicine for providing MCF7/neo and MCF7/HER2-18 cell lines and Dr. Pang-Kuo Lo for technical assistance on FACS analysis. This work was supported by the American Cancer Society Research Award (RSG-10-067-01-TBE) and NIH grant (1R01CA178386) to HC, by NSF grant

(DMS1019544) to XL, by NIH grants (R01GM67247 and P50GM76516) and NSF grant (DMS 1161621) to QN, and by NSF grant (DMS-0908330, DMS-1200487, CMMI-0849317) and NIH grant (2R01GM078994-05A1) to QW¹ and a SC/EPSCOR GEAR award to QW¹ and XL.

Author contributions

X.L., Q.W.¹ and Q.N. developed mathematical models, analysis and performed simulations. H.C., Q.W.³, S.J., D.K., W.Y. and U.S. performed the biological experiments and analyzed the data. H.C. and X.L. wrote the paper.

Additional information

Supplementary information accompanies this paper at <http://www.nature.com/scientificreports>

Competing financial interests: The authors declare no competing financial interests.

How to cite this article: Liu, X. F. *et al.* Nonlinear Growth Kinetics of Breast Cancer Stem Cells: Implications for Cancer Stem Cell Targeted Therapy. *Sci. Rep.* **3**, 2473; DOI:10.1038/srep02473 (2013).



This work is licensed under a Creative Commons Attribution-NonCommercial-ShareAlike 3.0 Unported license. To view a copy of this license, visit <http://creativecommons.org/licenses/by-nc-sa/3.0>



DOI: 10.1038/srep03173

SUBJECT AREAS:
APPLIED MATHEMATICS
BREAST CANCER
CANCER MODELS
CANCER STEM CELLS

CORRIGENDUM: Nonlinear Growth Kinetics of Breast Cancer Stem Cells: Implications for Cancer Stem Cell Targeted Therapy

Xinfeng Liu, Sara Johnson, Shou Liu, Deepak Kanojia, Wei Yue, Udai P. Singh, Qian Wang, Qi Wang,
Qing Nie & Hexin Chen

The original version of this Article contained a typographical error in the spelling of the author Udai P Singh, which was incorrectly given as Udai Singn. This has now been corrected in both the PDF and HTML versions of the Article.

SCIENTIFIC REPORTS:
3 : 2473
DOI: 10.1038/srep02473
(2013)

Published:
20 August 2013

Updated:
12 November 2013